

# Cu(II) adsorption from copper mine water by chitosan films and the matrix effects

Tuanny S. Frantz<sup>1</sup> · Nauro Silveira Jr.<sup>1</sup> · Maurício S. Quadro<sup>2</sup> · Robson Andreazza<sup>2</sup> · Amauri A. Barcelos<sup>2</sup> · Tito R. S. Cadaval Jr.<sup>1</sup> · Luiz A. A. Pinto<sup>1</sup>

Received: 3 December 2016 / Accepted: 26 December 2016 / Published online: 7 January 2017  
© Springer-Verlag Berlin Heidelberg 2017

**Abstract** Adsorption of copper ions onto chitosan films was studied, and the matrix effect was evaluated using a synthetic solution and a real effluent from closed copper mine. Chitosan films were prepared by casting technique and characterized. The adsorption study was carried out by equilibrium isotherms, thermodynamics, and kinetics. The thermodynamic parameters indicated that the copper adsorption onto chitosan film was favorable, spontaneous, and exothermic, suggesting an increased randomness at the solid/solution interface. The matrix effect was evaluated in kinetic assays, where a synthetic solution and a real system were carried out at different stirring rates. The highest values of adsorption capacity

reached in all stirring rates were about 20% lower in the real effluent, and this reduction in the competitiveness was due to the presence of other ions in the matrix of the real effluent. The maximum adsorption capacity of copper ions onto chitosan films for the synthetic solution was of 450 mg g<sup>-1</sup>, and the removal percentage was in the range from 78 to 96%, and these values for the real effluent were of 360 mg g<sup>-1</sup> and removal ranging from 62 to 76%. The mapping done of ions present in the water adsorbed of the mine in the films showed that the same was homogeneously distributed in the films' surfaces.

Responsible editor: Guilherme L. Dotto

✉ Luiz A. A. Pinto  
dqmpinto@furg.br

Tuanny S. Frantz  
tuanny.frantz@gmail.com

Nauro Silveira, Jr.  
nauroeq@yahoo.com.br

Maurício S. Quadro  
mausq@hotmail.com

Robson Andreazza  
robsonandreazza@yahoo.com.br

Amauri A. Barcelos  
aabarcelos@gmail.com

Tito R. S. Cadaval, Jr.  
titoeq@gmail.com

<sup>1</sup> School of Chemistry and Food, Federal University of Rio Grande (FURG), FURG, km 8 Itália Avenue, Carreiros District, Rio Grande, RS, Brazil

<sup>2</sup> Engineering Department, Federal University of Pelotas (UFPEl), Pelotas, RS, Brazil

**Keywords** Adsorption · Chitosan film · Copper ions · Matrix effect · Wastewater

## Introduction

Practices of water reuse reduce the costs associated with pollution and contribute to environmental protection and public health. Based on the guidelines adopted by the Economic and Social Council of the United Nations (ONU), no good quality water should be used in activities that tolerate lower quality water. Thus, the reuse of water constitutes practice rationalization and conservation of water resources. In this context, removal of heavy metals from industrial effluents has great importance due to rigorous environmental standards. There are many industrial effluents containing different metal ions which currently contribute to environmental pollution (Ali and Jain 2004; Feng et al. 2000; Hunsom et al. 2005; Matlock et al. 2002). The extractive metallurgy activity is a strong polluter process, which contaminates the surrounding soil and the surface water streams with its wastewater, where one of the most reported ions presented in wastewater is the Cu(II), with a maximum contaminant level in industrial

effluents around  $1.3 \text{ mg L}^{-1}$ . Wastewater originating from active or closed copper mines is extremely dangerous to the environment for a very long period of time (Crini and Badot 2008). The water flow of the copper mines can reach several cubic meters per minute, and these wastewaters can lead to environmental problems such as groundwater contamination and adjacent rivers (Geets et al. 2006).

Treatment processes, such as extraction, resins, and electrokinetics, are not economically viable to removal of ions from aqueous medium (Dotto et al. 2013; Guibal 2004). In this way, adsorption is considered to be one interesting method (Ali 2014; Ali et al. 2012; Crini and Badot 2008). Activated carbon is the most common adsorbent used to remove heavy metals; however, several alternative adsorbents has been researched. Chitosan, a linear biopolymer of acetylamino-D-glucose obtained from chitin alkaline deacetylation, has shown promising due to its high content of amino and hydroxyl groups, which have elevated potential for interaction with pollutants (Cadaval Jr. et al. 2013; Crini and Badot 2008; Wang et al., 2016 )

Chitosan films are suitable for removal of heavy metals from aqueous solutions due to its the mechanical properties, as tensile strength, elongation, and swelling properties (Batista et al. 2011; Fajardo et al. 2012; Tao et al. 2009; Vieira et al. 2011), and they are applicability in a wide range of pH (Fajardo et al. 2012). The literature showed that chitosan films were effective to remove various heavy metals from aqueous solutions (Batista et al. 2011; Cadaval et al. 2015; Tao et al. 2009; Vieira et al. 2011; Yamani et al. 2016; Yavuz et al. 2003). However, there is little information about the removal of metal ions from a real effluent by adsorption using chitosan films.

This work aimed on the removal of Cu(II) from both a synthetic solution which contained a single ionic specie and a mine water (real) having different ions present. Chitosan films (CFs) were prepared by casting technique and characterized. After, the equilibrium, thermodynamic, and kinetic studies of the mine water and of the synthetic solution to identify the influence of the matrix in the adsorption operation were performed.

## Material and methods

### Preparation and characterization of chitosan films

Chitosan was obtained from shrimp wastes (*Penaeus brasiliensis*) according to the procedure developed by Moura et al. (2011) (molecular weight of  $150 \pm 3 \text{ kDa}$ , deacetylation degree of  $85 \pm 1\%$ , and medium diameter of  $70 \pm 5 \mu\text{m}$ ). CFs were produced by casting technique, as detailed in our previous work (Dotto et al. 2011). The tensile strength and elongation of the CF were measured by a texture analyzer (Stable

Micro Systems, TA-XT-2i, UK) with a 50 N load cell. The testing speed for texture analysis was  $2 \text{ mm s}^{-1}$ . The CF thicknesses were measured before and after the adsorption process by a digital micrometer (Insize, IP54, Brazil) with  $0.0010 \text{ mm}$  of resolution (ASTM 2001).

After adsorption, the CFs were analyzed by SEM/EDS mapping of adsorbed ions. The analyzes were performed using a scanning electron microscope (JEOL JSM 6610LV, Japan) with energy-dispersive probe X-ray (Goldstein et al. 2003). The samples were metalized with carbon on vacuum chamber (Denton Vacuum, Sputtering Desk V, USA) and were used with acceleration voltage of 15 kV to obtain the images and mapping. The alterations in the functional groups due to the adsorbate–adsorbent interactions were identified by FT-IR (Prestige, 21210045, Japan) using diffuse reflectance in KBr pellets (Silverstein et al. 2005).

### Adsorption assays

For the synthetic solution, a copper stock solution ( $1 \text{ g L}^{-1}$ ) was prepared with  $\text{CuSO}_4 \cdot 5\text{H}_2\text{O}$  (purity of 99.0%) (Merck, Germany), and all samples of the synthetic solution were elaborated by diluting this one. The pH was adjusted using buffer disodium phosphate/citric acid solution  $0.1 \text{ mol L}^{-1}$ , and it was measured before and after the adsorption by a pH meter (Mars, MB10, Brazil). For all the assays, CFs were divided in portions ( $1 \times 1 \text{ cm}$ ). The adsorption assays were carried out for the equilibrium and thermodynamic studies in batch process, at 100 rpm and in temperatures of 298, 308, 318, and 328 K, with pH 6, the film dosage of  $250 \text{ mg L}^{-1}$ , and the copper concentration from 25 to  $250 \text{ mg L}^{-1}$ . The kinetic assays were performed at 50, 100, and 200 rpm; the film dosages were of  $100 \text{ mg L}^{-1}$ , and the copper concentrations were adjusted at  $50 \text{ mg L}^{-1}$ , for both the synthetic solution and the mine water (which had different ion mixtures).

The initial concentrations of the mine water samples were measured by atomic absorption spectrometry with flame (GBC Avanta, 932AA, Australia). The equilibrium adsorption capacity ( $q_e$ ) and adsorption capacity at time  $t$  ( $q_t$ ) were determined by Eqs. (1) and (2):

$$q_e = \frac{V(C_0 - C_e)}{m} \quad (1)$$

$$q_t = \frac{V(C_0 - C_t)}{m} \quad (2)$$

where  $C_0$  is the initial copper concentration in liquid phase ( $\text{mg L}^{-1}$ ),  $C_e$  is the equilibrium copper concentration in liquid phase ( $\text{mg L}^{-1}$ ),  $C_t$  is the copper concentration in liquid phase at time  $t$  ( $\text{mg L}^{-1}$ ),  $m$  is amount of chitosan (g), and  $V$  is the volume of solution (L).

## Equilibrium and thermodynamic studies

The equilibrium conditions and thermodynamic parameters of the adsorption process are extensively studied by adsorption models. The isotherm models Henry and Freundlich were used to fit the experimental data obtained at 298, 308, 318, and 328 K.

The model Henry model is used when the relationship between the amount of adsorbate in the fluid phase and the amount of adsorbate on the solid phase is linear, being the proportionality constant called of Henry's equilibrium constant ( $K_H$ ), represented by Eq. (3) (Ruthven 1984):

$$q_e = k_H C_e \quad (3)$$

The Freundlich model assumes that the surface is heterogeneous and can be represented by Eq. (4) (Ruthven 1984).

$$q_e = k_F C_e^{1/n} \quad (4)$$

where  $k_F$  is the Freundlich constant ( $(\text{mg g}^{-1})(\text{mg L}^{-1})^{-1/n}$ ) and  $1/n$  is the heterogeneity factor.

The thermodynamic parameters, such as Gibb's free energy change ( $\Delta G^0$ ), for the copper adsorption by CF were determined by Eq. (5).

$$\Delta G^0 = -RT \ln(\rho_w K_D) \quad (5)$$

where  $K_D$  is the thermodynamic equilibrium constant ( $\text{L g}^{-1}$ ),  $\rho_w$  is the water density ( $\text{g L}^{-1}$ ),  $T$  is the temperature (K), and  $R$  is the universal gas constant ( $8.314 \text{ J mol}^{-1} \text{ K}^{-1}$ ) (Liu 2009).

The enthalpy change ( $\Delta H^0$ ) ( $\text{kJ mol}^{-1}$ ) and entropy change ( $\Delta S^0$ ) ( $\text{kJ mol}^{-1} \text{ K}^{-1}$ ) were determined by Van't Hoff's plot, according to Eq. (6) (Ruthven 1984):

$$\ln(\rho_w K_D) = \frac{\Delta S^0}{R} - \frac{\Delta H^0}{RT} \quad (6)$$

## Kinetic models

The kinetic data were evaluated at different stirring rates (from 50 to 200 rpm) by pseudo-first-order, pseudo-second-order, and Elovich models.

The kinetic models of pseudo-first order and pseudo-second order assume that adsorption is a pseudo-chemical reaction, and the adsorption rate can be determined, respectively, by Eqs. (7) and (8) (Ruthven 1984; Dotto and Pinto 2011):

$$q_t = q_1 (1 - \exp(-k_1 t)) \quad (7)$$

$$q_t = \frac{t}{(1/k_2 q_2^2) + (t/q_2)} \quad (8)$$

where  $k_1$  and  $k_2$  are the rate constants of pseudo-first-order and pseudo-second-order models, respectively, in  $\text{min}^{-1}$  and

$\text{g mg}^{-1} \text{ min}^{-1}$ ,  $q_1$  and  $q_2$  are the theoretical values for the adsorption capacity ( $\text{mg g}^{-1}$ ), and  $t$  is the time (min).

The Elovich kinetic model is described by Eq. (9) (Ruthven 1984; Dotto and Pinto 2011):

$$q_t = \frac{1}{a} \ln(1 + abt) \quad (9)$$

where  $a$  is the initial sorption rate due to  $dq/dt$  with  $q_t = 0$  ( $\text{mg g}^{-1} \text{ min}^{-1}$ ) and  $b$  is the desorption constant of the Elovich model ( $\text{g mg}^{-1}$ ).

The removal percentage (%R) was calculated by Eq. (10):

$$\%R = \frac{C_0 - C_t}{C_0} \times 100 \quad (10)$$

Kinetic and isotherm parameters were estimated by nonlinear regression using Statistica 7.0 software (Statsoft, USA). Objective function was quasi-Newton. The fit quality was evaluated by determination coefficient ( $R^2$ ), adjusted determination coefficient ( $R^2_{adj}$ ) Eq. (11), and average relative error (ARE) Eq. (12):

$$R^2_{adj} = 1 - (1 - R^2) \left( \frac{N-1}{N-p} \right) \quad (11)$$

where  $N$  is the number of experimental points and  $p$  is the parameter number of the model.

$$\text{ARE} = \frac{100}{n} \sum_1^n \left| \frac{q_{\text{exp}} - q_{\text{pre}}}{q_{\text{exp}}} \right| \quad (12)$$

where  $q_{\text{exp}}$  and  $q_{\text{pre}}$  are the adsorption capacity values experimental and theoretical, respectively, obtained from the models.

## Results and discussion

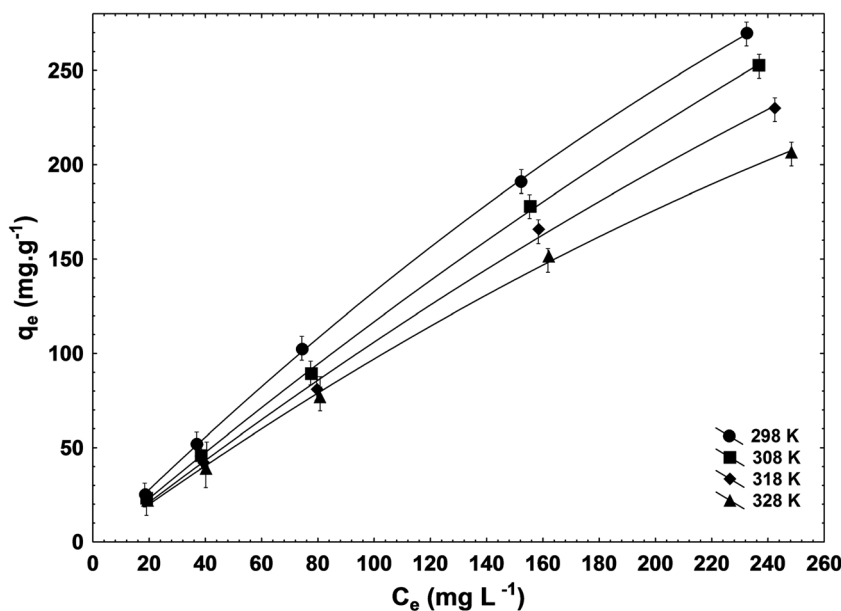
### Chitosan film characteristics

The chitosan films were characterized according to the mechanical properties and thickness. CF samples presented tensile strength of  $28.3 \pm 2.0$  MPa, elongation of  $12.2 \pm 1.5\%$ , and thicknesses of  $62 \pm 3$   $\mu\text{m}$ . Thus, the CF samples showed good mechanical properties, being suitable for use in adsorption operation (Dotto et al. 2011; Vieira et al. 2011), facilitating the phase separation after the operation (Fajardo et al. 2012).

### Equilibrium and thermodynamic

The Figure 1 shows the temperature effect in adsorption equilibrium of copper onto CF. The adsorption equilibrium isotherms were obtained at 298, 308, 318, and 328 K. The assays

**Fig. 1** Effect of temperature on copper adsorption equilibrium onto chitosan film (CF)



were characterized by a linear increase in adsorption capacity when the copper concentration increased, showing a constant partition of the adsorbate in both phases in all the copper concentration range. This compartment indicates a great CF–copper affinity and that the monolayer is not yet saturated. Only at 328 K, a tendency of convex shape can be observed, which suggests the initial saturation of the monomolecular layer of the copper onto CF surface (Gerente et al. 2007). Furthermore, it was verified that the adsorption capacity increased with the decrease in temperature, reaching maximum values at 298 K (270 mg g<sup>-1</sup>), and the isotherm profile was similar to the Henry’s law. This occurred because the temperature increase leads to an increase in the copper ion solubility;

thus, the interaction of the desolvation forces becomes stronger. Henry and Freundlich isotherm models were employed to obtain information about the equilibrium curves. The isotherm parameters for the adsorption are shown in Table 1. The high values of determination coefficient ( $R^2 > 0.99$ ) and adjusted determination coefficient ( $R^2_{adj} > 0.99$ ) and the low values of

**Table 1** Isotherm parameters for copper adsorption onto chitosan film (CF)

Model	298 K	308 K	318	328 K
<b>Henry</b>				
$k_H$ (L g <sup>-1</sup> )	1.204	1.096	0.982	0.871
$R^2$	0.991	0.996	0.994	0.988
$R^2_{adj}$	0.991	0.996	0.994	0.988
ARE (%)	8.9	5.7	7.3	10.5
<b>Freundlich</b>				
$k_F$ (mg g <sup>-1</sup> )(L mg <sup>-1</sup> ) <sup>-1/n</sup>				
$n$	1.14	1.08	1.09	1.14
$R^2$	0.999	0.999	0.997	0.997
$R^2_{adj}$	0.999	0.999	0.996	0.996
ARE (%)	5.4	3.2	3.7	4.3

**Table 2** Adsorption results of copper(II) ions using different adsorbents

Adsorbent	Adsorption capacity (mg g <sup>-1</sup> )	pH	Reference
Orange peels	3.65	6–8	Annadural et al. (2002)
Banana peels	4.70	6–8	Annadural et al. (2002)
<i>Lyngya putealis</i>	7.75	6	Kiran and Thanasekaran (2011)
Vermiculite	20.61	6	Ulmanu and Fernandez (2003)
Kaolinite	10.79	–	Yavuz et al. (2003)
Epichlorohydrin cross-linked xanthate chitosan	43.47	5	Kannamba et al. (2010)
Chitosan immobilized on bentonite	23.11	4–6	Futalan et al. (2011)
Chitosan films	270.00	6	Current research

**Table 3** Thermodynamic parameters for the copper adsorption onto chitosan film (CF)

Temperature (K)	$\Delta G^0$ (kJ mol <sup>-1</sup> ) <sup>a</sup>	$\Delta H^0$ (kJ mol <sup>-1</sup> ) <sup>a</sup>	$\Delta S^0$ (kJ mol <sup>-1</sup> K <sup>-1</sup> ) <sup>a</sup>
298	-17.44 ± 0.01	-8.86 ± 0.15	0.03 ± 0.01
308	-17.84 ± 0.03		
318	-18.12 ± 0.01		
328	-11.30 ± 0.02		

<sup>a</sup> Mean ± standard deviation ( $n = 3$ )

average relative error (ARE < 5.5%) showed that the Freundlich model was the more suitable to fit the equilibrium data; however, the values of the heterogeneity factor ( $1/n$ ) suggest a low difference of energy in the sites present in adsorbent surface.

The adsorption capacity of the copper ions onto chitosan film was from 270 mg g<sup>-1</sup> at 298 K. This result demonstrates the great potential of chitosan films, and when compared to other adsorbents of the literature (Table 2), it shows a high adsorption capacity.

The adsorption thermodynamic study was realized through the estimation of Gibbs free energy change, enthalpy change, and entropy change. These parameters for the adsorption of copper ions onto CF are shown in Table 3. The negative values of  $\Delta G^0$  indicate that the adsorption was a spontaneous and favorable process at all the studied temperatures (Ge and Li 2011). The enthalpy changes ( $\Delta H^0$ ) indicate that adsorption was an exothermic process. In addition, the magnitude of enthalpy was consistent with electrostatic interactions. This is an indicative that electrostatic coordination occurred between the unprotonated amine and hydroxyl groups of the chitosan films and the ions Cu<sup>2+</sup>, since this kind of interaction dominates in less acidic solutions (Guibal 2004). The positive values of  $\Delta S^0$  indicate that randomness increased at the solid–solution interface during the adsorption (Ge and Li 2011).

### Kinetics and matrix effects

The adsorption kinetics of the pure copper solution (synthetic solution) and the mine water (real system) were studied, and

**Table 4** Concentrations of same elements from the copper mine water

Element	Cu	Al	S	Fe	Ca	Cr	Ni
C (g L <sup>-1</sup> )	43.12	3.84	112.32	3.87	35.32	0.09	0.02

**Table 5** Kinetic parameters for copper adsorption from the synthetic solution

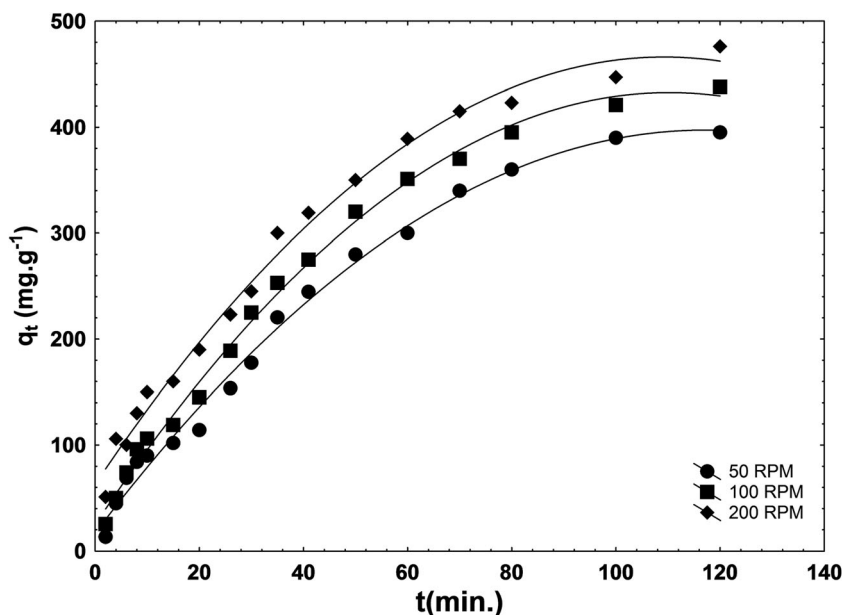
Kinetic model	Stirring rate (rpm)		
	50	100	200
Pseudo-first order			
$q_1$ (mg g <sup>-1</sup> )	461.9	449.3	463.7
$k_1$ (min <sup>-1</sup> )	0.018	-0.024	0.030
$R^2$	0.988	0.989	0.972
ARE (%)	4.2	5.0	4.8
Pseudo-second order			
$q_2$ (mg g <sup>-1</sup> )	675.5	621.7	603.3
$k_2$ (g mg <sup>-1</sup> min <sup>-1</sup> )	4,095,287	4,749,533	6,098,709
$R^2$	0.986	0.995	0.991
ARE (%)	2.5	1.4	1.8
Elovich			
$a$ (g mg <sup>-1</sup> )	0.004	0.005	0.006
$b$ (mg g <sup>-1</sup> min <sup>-1</sup> )	9.96	14.35	22.17
$R^2$	0.985	0.979	0.977
ARE (%)	5.2	5.5	5.0

the pseudo-first-order, pseudo-second-order, and Elovich models were used to describe the kinetic data. The initial ion concentrations of the mine water sample are in the Table 4. Among the adjusted models, in both samples, the pseudo-

**Table 6** Kinetic parameters for copper adsorption from the real system (mine water)

Kinetic model	Stirring rate (rpm)		
	50	100	200
Pseudo-first order			
$q_1$ (mg g <sup>-1</sup> )	315.8	334.6	338.9
$k_1$ (min <sup>-1</sup> )	0.038	0.044	0.057
$R^2$	0.981	0.982	0.985
ARE (%)	3.2	2.9	3.3
Pseudo-second order			
$q_2$ (mg g <sup>-1</sup> )	399.9	414.3	404.0
$k_2$ (g mg <sup>-1</sup> min <sup>-1</sup> )	2,376,786	3,244,934	4,268,424
$R^2$	0.995	0.996	0.990
ARE (%)	2.4	1.4	2.6
Elovich			
$a$ (g mg <sup>-1</sup> )	0.009	0.010	0.011
$b$ (mg g <sup>-1</sup> min <sup>-1</sup> )	19.99	27.08	42.67
$R^2$	0.987	0.989	0.96
ARE (%)	3.4	2.8	4.8

**Fig. 2** Kinetic curves of copper ions in the synthetic solution



second-order model showed better fit than the other ones. Tables 5 and 6 show the values of determination coefficient ( $R^2$ ) and ARE for the synthetic solution and the real system, respectively.

Several studies for adsorption of divalent metals reported that the majority of the metal sorption kinetics follows pseudo-second-order mechanisms (Ho 2006; Wu et al. 2001). In Figs. 2 and 3 can be observed that the maximum values of adsorption capacity in the synthetic

solution were about 20% higher than in the real effluent in the same time interval (120 min). Another change which may be observed due to the presence of other ions in solution is the rate at which copper was adsorbed. In Fig. 2 (synthetic solution), the slope of the linear portion of the kinetic curves extends for a longer period of time (around 70 min). However, the values observed in Fig. 3 for copper adsorption from the real matrix showed a short period of time (around

**Fig. 3** Kinetic curve of ion copper ions in the real system (mine water)

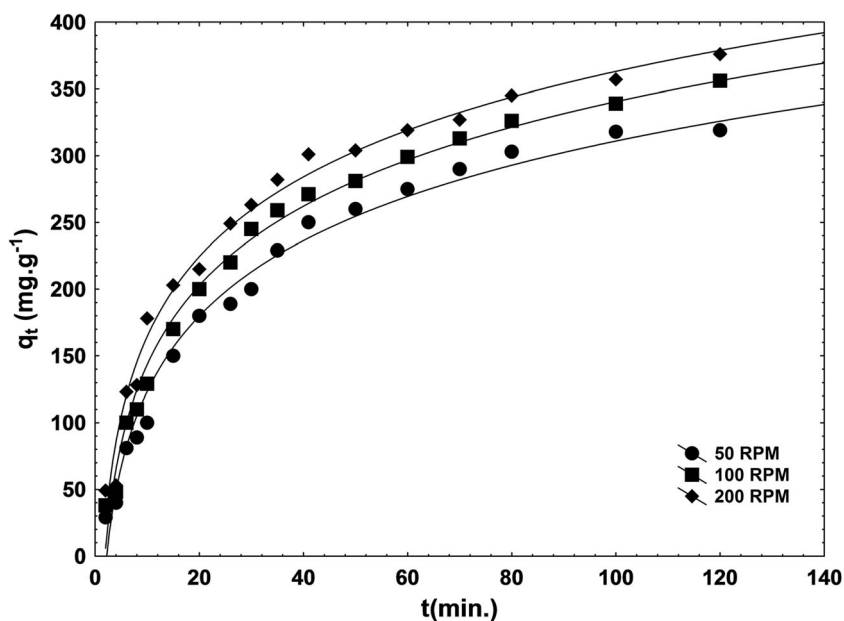


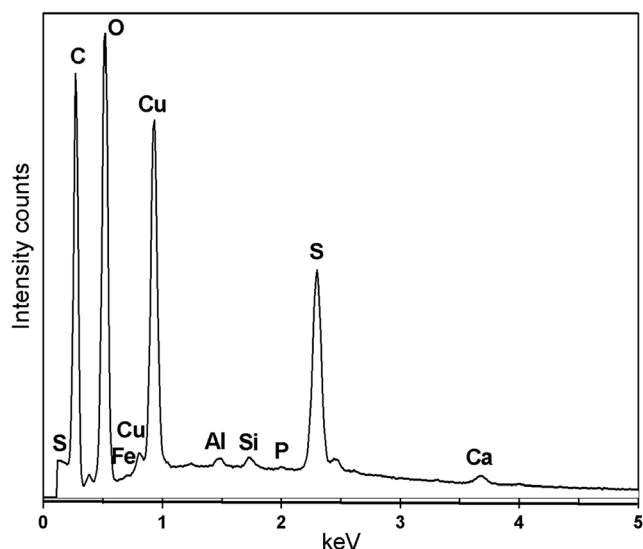
**Table 7** Removal percentage of the copper ions onto chitosan films (CF)

Stirring rate (rpm)	%R
Synthetic solution	
50	78
100	88
200	96
Mine water	
50	62
100	72
200	76

30 min) of the linear portion. This difference in Figs. 2 and 3 can be attributed to the competitiveness due to the presence of other ions in the matrix, which occupy some sites that would be filled by copper ions in the absence of the same. Thus, the monolayer of adsorbent was filled faster because there are other molecules competing for the same active site. The existence of other ions increases the steric hindrance, since the occurrence of complexes can generate retention of more than one type of element in each active site in a given time interval. The removal percentage values of the copper ions are shown in Table 7.

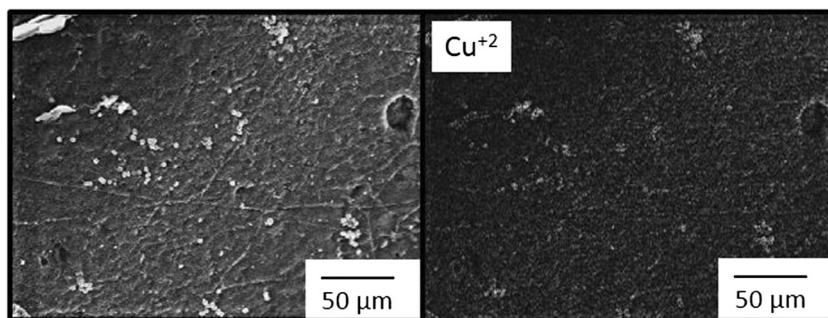
The EDS spectrum of the film after adsorption is shown in Fig. 4, which presents the characteristic elements of the groups of CF, as also the ions present in mine water adsorbed in the film. It was carried out a mapping of the ions adsorbed on the synthetic solution and on the mine water, which are shown in Figs. 5 and 6, respectively, where their distributions in the CF can be observed.

In the synthetic solution, the copper ions were adsorbed homogeneously in the film (Fig. 5). In the mine water, the copper ions also were absorbed evenly; however, there were other ions which occupied sites of the adsorbent, such as Al, S, Fe, and Ca (Fig. 6). Through these images, it can be said that the active sites of CF are homogeneous once all mapped ions

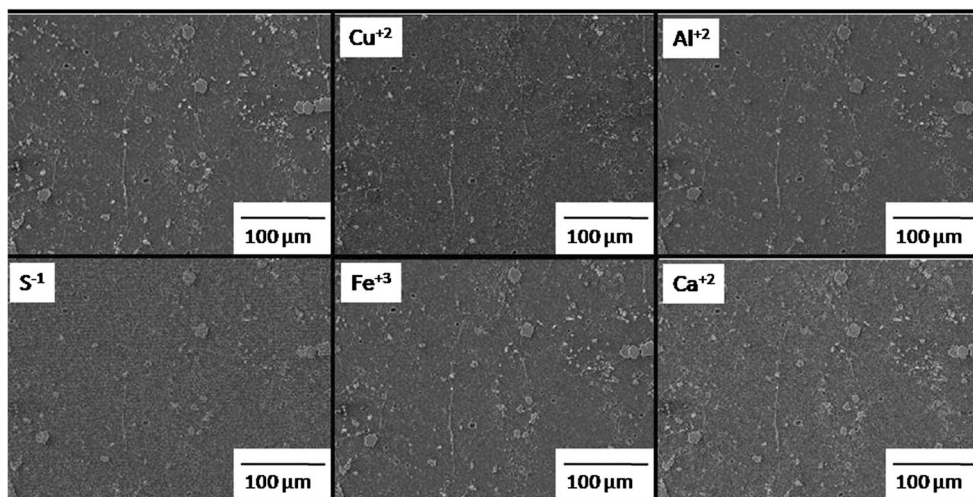
**Fig. 4** EDS spectrum of CF after adsorption of ions present in the mine water

were distributed homogeneously. Although this reduction occurs, the copper ions were able to compete well by the active sites. It is possible that the interaction of the copper ions has been sustained by the stronger binding, which resulted only in a small reduction in the adsorption efficacy of these ions when compared to the synthetic solution. This effect suggested that the amino group was deprotonated in pH 6 and the mechanism between chitosan and copper ions was superior to other adsorption mechanism when more ions are present (Hasan et al. 2008; Jeon and Höll 2003).

Figure 7 shows FT-IR analysis of pure chitosan films, chitosan films adsorbed with copper ions, and chitosan films adsorbed with copper ions from mine water. Changes in both film spectrums after the adsorption assays when compared to the spectrum of pure chitosan films can be observed. The bands associated to the N–H and O–H stretching (between 3600 and 3200  $\text{cm}^{-1}$ ) of the biopolymer were altered due to the interaction between these

**Fig. 5** Mapping of ions present in the synthetic solution adsorbed onto CF

**Fig. 6** Mapping of ions present in the mine water adsorbed onto CF

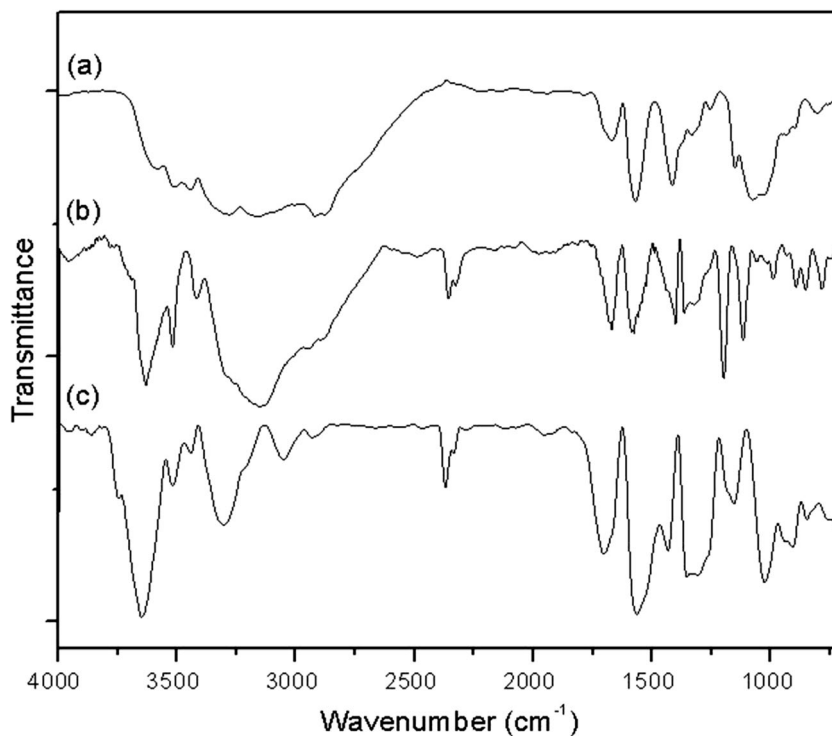


functional groups and the ions present in the solution. The major differences in the spectrum of the real effluent can be observed around  $1000\text{ cm}^{-1}$  relative to C–N and C–O stretching (Cadaval Jr. et al. 2013). These changes can be attributed to the interactions of the other ions present in the matrix, since each adsorbate can to interact at different way in the chitosan structure.

Thus, the most prominent result here is the maintaining of a high adsorption capacity of the copper in a

complex matrix in spite of the presence of other ions, when compared with a synthetic solution of the copper ions. The difference of the values can be seen at the kinetic behavior, where the maximum capacity of adsorption reached  $450\text{ mg g}^{-1}$  in the synthetic solution and  $360\text{ mg g}^{-1}$  for the real effluent (mine water) in the same time interval. These results suggest that the chitosan film preserves the efficiency in the treatment of wastewater containing many different ions.

**Fig. 7** FT-IR analysis of **a** pure chitosan films, **b** chitosan films adsorbed with copper ions, and **c** chitosan films adsorbed with copper ions from mine water





## Conclusion

This work evaluated the effect of the matrix of a real effluent in the adsorption kinetics of copper ions by chitosan films. At the same time, studies of kinetics, equilibrium, and thermodynamic were performed using solutions containing only copper ions (synthetic model). The CF presented tensile strength of  $28.3 \pm 2.0$  MPa, elongation of  $12.2 \pm 1.5\%$ , and film thickness of  $70 \pm 5$   $\mu\text{m}$ . The Freundlich model presented the best fit to represent the equilibrium adsorption isotherms of the synthetic solutions, and the adsorption was spontaneous and exothermic, and an increased randomness at the solid/solution interface occurred. The pseudo-second-order equation showed better fit than the other ones for both the synthetic solutions and real effluent. The highest values of adsorption capacity in the synthetic solutions were about 20% higher than in the real effluent (maximum adsorption capacity for the synthetic solution was of  $450 \text{ mg g}^{-1}$ , and the real effluent was of  $360 \text{ mg g}^{-1}$ ). This difference in adsorption capacities was due to the presence of other ions adsorbed, as shown by mapping where the ions were homogeneously distributed in the adsorbent. The EDS spectrum showed the presence of groups of chitosan and the different ions present in the mine water. In the spectrums of the FT-IR, changes were observed in the bands associated to the functional groups of the biopolymer, and this was due to the interactions between these sites of the biopolymer and the ions present in the solution. The linear portion of the kinetic conducted with synthetic solutions were extended for a period longer than in to the real effluent. Although of the competitive medium and of an effect of the steric hindrance, the adsorption capacity values showed that the chitosan film maintained the efficiency in the treatment of the wastewater containing copper ions, once 80% of the adsorption capacity was reached in the real system when compared with the synthetic solution (the maximum values of removal percentage for the copper ions of the synthetic solution and the real effluent were of 96 and 76%, respectively).

**Acknowledgements** The authors would like to thank CAPES (Brazilian Agency for Improvement of Graduate Personnel) and CNPq (National Council of Science and Technological Development) for the financial support and CEME-Sul/FURG for SEM images and EDS.

## References

- Ali I (2014) Water treatment by adsorption columns: evaluation at ground level. *Sep Purif Rev* 43:175–205. doi:10.1080/15422119.2012.748671
- Ali I, Asim M, Khan TA (2012) Low cost adsorbents for the removal of organic pollutants from wastewater. *J Environ Manag* 113:170–183. doi:10.1016/j.jenvman.2012.08.028
- Ali I, Jain CK (2004) Advances in arsenic speciation techniques. *Int J Environ Anal Chem* 84:947–964. doi:10.1080/03067310410001729637
- ASTM (2001) American Society for Testing and Materials. Standard test methods for tensile properties of thin plastic sheeting (Standard D882–02, 162–170), Philadelphia.
- Annadural G, Juang RS, Lee DJ (2002) Adsorption of heavy metals from water using banana and orange peels. *Water Sci Technol* 47:185–190
- Batista ACL, Villanueva ER, Amorim RVS, Tavares MT, Campos-Takaki GM (2011) Chromium(VI) ion adsorption features of chitosan film and its chitosan/zeolite conjugate 13X film. *Molecules* 16:3569–3579. doi:10.3390/molecules16053569
- Cadaval TRS, Dotto GL, Seus ER, Mirlean N, Pinto LAA (2015) Vanadium removal from aqueous solutions by adsorption onto chitosan films. *Desalin Water Treat* 3994:1–9. doi:10.1080/19443994.2015.1079741
- Cadaval TRS Jr, Camara AS, Dotto GL, Pinto LAA (2013) Adsorption of Cr(VI) by chitosan with different deacetylation degrees. *Desalin Water Treat* 51:37–41. doi:10.1080/19443994.2013.778797
- Crini G, Badot PM (2008) Application of chitosan, a natural aminopolysaccharide, for dye removal from aqueous solutions by adsorption processes using batch studies: a review of recent literature. *Prog Polym Sci* 33:399–447. doi:10.1016/j.progpolymsci.2007.11.001
- Dotto GL, Souza VC, Moura JM, Moura CM, Pinto LAA (2011) Influence of drying techniques on the characteristics of chitosan and the quality of biopolymer films. *Dry Technol* 29:1784–1791. doi:10.1080/07373937.2011.602812
- Dotto GL, Moura JM, Cadaval TRS, Pinto LAA (2013) Application of chitosan films for the removal of food dyes from aqueous solutions by adsorption. *Chem Eng J* 214:8–16. doi:10.1016/j.cej.2012.10.027
- Dotto GL, Pinto LAA (2011) Adsorption of food dyes acid blue 9 and food yellow 3 onto chitosan: stirring rate effect in kinetics and mechanism. *J Hazard Mater* 187:164–170. doi:10.1016/j.jhazmat.2011.01.016
- Fajardo AR, Lopes LC, Rubira AF, Muniz EC (2012) Development and application of chitosan/poly(vinyl alcohol) films for removal and recovery of Pb(II). *Chem Eng J* 183:253–260. doi:10.1016/j.cej.2011.12.071
- Feng D, Aldrich C, Tan H (2000) Treatment of acid mine water by use of heavy metal precipitation and ion exchange. *Miner Eng* 13:623–642. doi:10.1016/S0892-6875(00)00045-5
- Futalan CM, Kan CC, Dalida ML et al (2011) Comparative and competitive adsorption of copper, lead, and nickel using chitosan immobilized on bentonite. *Carbohydr Polym* 83:528–536. doi:10.1016/j.carbpol.2010.08.013
- Ge P, Li F (2011) Kinetics and thermodynamics of heavy metal Cu(II) adsorption on mesoporous silicates. *Polish J Environ Stud* 20:339–344
- Geets J, Vanbroekhoven K, Borremans B, Vangronsveld J, Diels L (2006) Column experiments to assess the effects of electron donors on the efficiency of in situ precipitation of Zn, Cd, Co and Ni in contaminated groundwater applying the biological sulfate removal technology. *Environ Sci Pollut Res* 13:362–378
- Gerente C, Lee VKC, Cloirec PL, McKay G (2007) Application of chitosan for the removal of metals from wastewaters by adsorption—mechanisms and models review. *Crit Rev Environ Sci Technol* 37:41–127. doi:10.1080/10643380600729089
- Goldstein J, Newbury DE, Joy DC, Lyman CE, Echlin P, Lifshin E, Sawyer L, Michael JR (2003) Scanning electron microscopy and X-ray microanalysis. Springer, New York
- Guibal E (2004) Interactions of metal ions with chitosan-based sorbents: a review. *Sep Purif Technol* 38:43–74. doi:10.1016/j.seppur.2003.10.004
- Hasan S, Ghosh TK, Viswanath DS, Boddu VM (2008) Dispersion of chitosan on perlite for enhancement of copper(II) adsorption capacity. *J Hazard Mater* 152:826–837. doi:10.1016/j.jhazmat.2007.07.078
- Ho YS (2006) Review of second-order models for adsorption systems. *J Hazard Mater* 136:681–689. doi:10.1016/j.jhazmat.2005.12.043
- Hunsom M, Pruksathorn K, Damronglerd S, Vergnes H, Duverneuil P (2005) Electrochemical treatment of heavy metals (Cu<sup>2+</sup>, Cr<sup>6+</sup>, Ni<sup>2+</sup>) from industrial effluent and modeling of copper reduction. *Water Res* 39:610–616. doi:10.1016/j.watres.2004.10.011

- Jeon C, Höll WH (2003) Chemical modification of chitosan and equilibrium study for mercury ion removal. *Water Res* 37:4770–4780. doi:10.1016/S0043-1354(03)00431-7
- Kannamba B, Reddy KL, AppaRao BV (2010) Removal of Cu(II) from aqueous solutions using chemically modified chitosan. *J Hazard Mater* 175:939–948. doi:10.1016/j.jhazmat.2009.10.098
- Kiran B, Thanasekaran K (2011) Copper biosorption on *Lyngbya putealis*: application of response surface methodology (RSM). *Int Biodeterior Biodegrad* 65:840–845. doi:10.1016/j.ibiod.2011.06.004
- Liu Y (2009) Is the free energy change of adsorption correctly calculated? *J Chem Eng Data* 54:1981–1985. doi:10.1021/je800661q
- Matlock MM, Howerton BS, Atwood DA (2002) Chemical precipitation of heavy metals from acid mine drainage. *Water Res* 36:4757–4764. doi:10.1016/S0043-1354(02)00149-5
- Moura CM, Moura JM, Soares NM, Pinto LAA (2011) Evaluation of molar weight and deacetylation degree of chitosan during chitin deacetylation reaction: used to produce biofilm. *Chem Eng Process Intensif* 50:351–355. doi:10.1016/j.cep.2011.03.003
- Ruthven DM (1984) Principles of adsorption and adsorption processes. John Wiley & Sons, New York
- Silverstein MR, Webster XF, Kiemle JD (2005) Spectrometric identification of organic compounds, 7th edn. John Wiley & Sons, New York
- Tao Y, Ye L, Pan J, Wang Y, Tang B (2009) Removal of Pb(II) from aqueous solution on chitosan/TiO<sub>2</sub> hybrid film. *J Hazard Mater* 161:718–722. doi:10.1016/j.jhazmat.2008.04.012
- Ulmanu M, Fernandez Y (2003) Removal of copper and cadmium ions from diluted aqueous solutions by low cost and waste material adsorbents. *Water Air Soil* 1:357–373
- Vieira RS, Oliveira MLM, Guibal E, Rodríguez-Castellón E, Beppu MM (2011) Copper, mercury and chromium adsorption on natural and crosslinked chitosan films: an XPS investigation of mechanism. *Colloids Surf A Physicochem Eng Asp* 374:108–114. doi:10.1016/j.colsurfa.2010.11.022
- Wang X, Liu Y, Zheng J (2016) Removal of As(III) and As(V) from water by chitosan and chitosan derivatives: a review. *Environ Sci Pollut Res* 23:13789–13801. doi:10.1007/s11356-016-6602-8
- Wu FC, Tseng RL, Juang RS (2001) Kinetic modeling of liquid-phase adsorption of reactive dyes and metal ions on chitosan. *Water Res* 35:613–618. doi:10.1016/S0043-1354(00)00307-9
- Yamani JS, Lounsbury AW, Zimmerman JB (2016) Towards a selective adsorbent for arsenate and selenite in the presence of phosphate: assessment of adsorption efficiency, mechanism, and binary separation factors of the chitosan-copper complex. *Water Res* 88:889–896. doi:10.1016/j.watres.2015.11.017
- Yavuz O, Altunkaynak Y, Guzel FG (2003) Removal of copper, nickel, cobalt and manganese from aqueous solution by kaolinite. *Water Res* 37:948–952. doi:10.1016/S0043-1354(02)00409-8